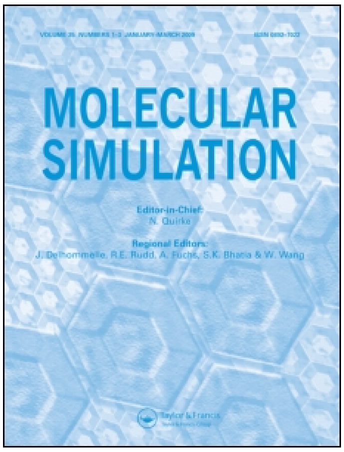

Molecular Simulation
Publication details, including instructions for authors and subscription information:
http://www.informaworld.com/smpp/title~content=t713644482

Molecular Dynamics Simulations of Polyacetylene

G. Sesé[ab]; C. R. A. Catlow[a]; B. Vessal[c]
[a] Davy Faraday Research Laboratory, The Royal Institution of GB, London, UK [b] Department de Física i Enginyeria Nuclear, Facultat d'Infor-màtica, UPC, Barcelona, Spain [c] Department of Chemistry, University of Keele, Keele, Staffordshire, UK

To cite this Article Sesé, G. , Catlow, C. R. A. and Vessal, B.(1992) 'Molecular Dynamics Simulations of Polyacetylene', Molecular Simulation, 9: 2, 99 — 113

To link to this Article: DOI: 10.1080/08927029208050604

URL: http://dx.doi.org/10.1080/08927029208050604

Molecular Simulation, 1992, Vol. 9, pp. 99–113
Reprints available directly from the publisher
Photocopying permitted by license only

MOLECULAR DYNAMICS SIMULATIONS OF POLYACETYLENE

G. SESÉ* and C.R.A. CATLOW

Davy Faraday Research Laboratory, The Royal Institution of GB,
21 Albemarle Street, London W1X 4BS, UK

and

B. VESSAL

Department of Chemistry, University of Keele, Keele, Staffordshire ST5 5BG, UK

(*Received April 1992; accepted April 1992*)

Molecular dynamics simulation methods have been used to study trans-polyacetylene both in its pristine and in its doped form. No constraints have been included in the simulations, so that both bond-lengths and bond-angles have been allowed to change. Bond energies, vibrational and structural data have been used to derive the potential parameters. The power spectra of the pristine polymer have been evaluated and they reproduce the main peaks observed in Raman and infrared experimental measurements. Doping by both lithium and potassium has been investigated at three different dopant levels. The results show that the mobility of the ions is remarkably high if their concentration is low. As the dopant level increases the displacements around the equilibrium positions become smaller and the dopants form an increasingly crystalline sublattice.

KEY WORDS: Polyacetylene, molecular dynamics

1 INTRODUCTION

It is well known that several conjugated polymers can conduct electricity after doping with oxidizing or reducing species, which modify the electronic structure of the polymer, resulting in a spectacular increase on its conductivity [1]. In the process of doping, mass transport plays an important role, but many questions concerning the mechanisms involved remain to be answered. Computer modelling can contribute to the understanding at a molecular level of this and other physical phenomena taking place in these and other polymers.

Atomistic simulations, based on static lattice methods and employing minimisation techniques have already been used to identify the most stable structures for the host polymers [2] and the lowest energy sites for the dopant ions [3]. In the present paper we extend the study to dynamical processes using the Molecular Dynamics simulation method (MD). We use standard microcanonical ensemble (NVE) MD, that is, we study the time evolution, under the laws of classical mechanics of systems of particles at constant volume interacting via conservative forces. As the available storage in the host computer and also the speed of execution of the program limit the size of the

---

Permanent address: Department de Fisica i Enginyeria Nuclear, Facultat d'Informàtica, UPC, Pau Gargallo 5, 08028 Barcelona, Spain.

systems, periodic boundary conditions [4] are considered, that is the sample under study is replicated throughout space to form an infinite lattice. In the simulation of chain molecules special attention has to be paid to the maintenance of the bonds across the boundaries of the system. In calculating the interatomic forces, the Minimum Image Convention [4] is considered for the short-range potentials. For the electrostatic interactions, the Ewald method [5] can be used to calculate in an efficient way the interaction of an ion or charged particle with all its periodic images.

Our calculations have focussed on polyacetylene (PA) [6], which is the archetype of electronically conducting polymers and has been used in a wide range of applications [7]. In this work, the trans-PA configuration has been analysed both in its pristine and in its doped form. Three different dopant levels have been considered, with both lithium and potassium as dopants.

Theoretical studies [8] suggest the existence of solitonic defects in PA. Charged solitons are supposed to play a fundamental role in the conductivity mechanism in lightly-doped PA. Their presence is also supported by experimental results [9] which note that both neutral and charged solitons may also play a role in the intermediate and heavy doped regimes. Nevertheless these defects are not taken into account in our simulations. We consider that this approximation will not alter significantly the results in the pristine and in the heavily doped polymer. The size of our system is small in the context of the density of solitons in the undoped material, which is about one every 1000–3000 carbon atoms [6]. The density of solitons is expected to be higher in the doped system. In heavily doped PA, a generalized soliton picture, involving delocalized carriers, appears to be implied by the combination of optical, magnetic and transport data [10]. This justifies the delocalisation of the charges assigned to the chains. This delocalisation is less realistic in the lightly doped system, but it can be useful to highlight the trends of the behaviour of such systems.

The organization of the remainder of this paper is as follows: The pristine system is studied in Section 2. In Section 3 we describe our work on the lightly doped polacetylene with lithium atoms. Section 4 is devoted to the potassium doped system, at two different dopant levels. A summary is given in Section 5.

2 PRISTINE POLYACETYLENE

2.1 Computational Details

The sample simulated comprises sixteen chains of PA each of them made up of six monomers. There are 384 atoms in the simulation box whose dimensions are 14.64 Å in the x direction, 16.96 Å in the y direction and 14.88 Å in the z direction. Due to the periodic boundary conditions, this generates an infinite system. The simulation started from the configuration referred to previously as the "out-of-phase" structure [11]. The corresponding unit cell is displayed in the Figure 1. The axis of all the chains are parallel to the z axis and the angle between the plane of a chain and the x axis has been set to 22°. The temperature of the system was 300 K. Newton's Second Law was solved numerically for every particle in the system using the leapfrog Verlet [12] algorithm. The integration timestep was of 10^{-15} s. A spherical molecular based cutoff with a radius equal to 7.32 Å was used to evaluate the interactions. The simulation consisted of a short initial equilibration period of 2 ps, which was found to be sufficient, and a production run of 150 ps.

The interatomic forces have been explicitly calculated using specified short range

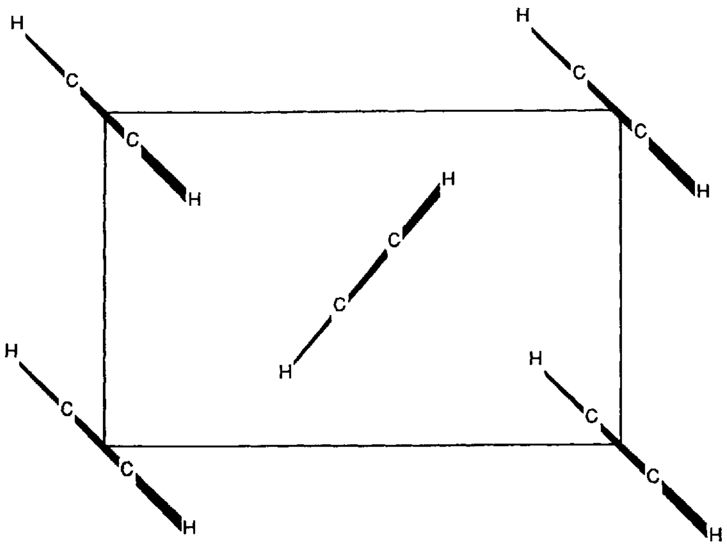

Figure 1 Unit cell of polyacetylene, projected normal to the chains directions (c axis). We define a as the longer of the two axes which are orthogonal to c (a = 7.32 Å, b = 4.24 Å, c = 4.96 Å).

potentials. No constraints have been included in the simulation, so that both bond-lengths and bond-angles have been allowed to vary. Morse (1) and harmonic potentials (2) control the bond lengths and the bond angles respectively. The non-bonded interactions are calculated using Buckingham-like potentials (3). They include all those between atoms located in different chains and those within the same chain provided that they are separated by three or more bonds as is customary practice [13]. As no torsional forces are considered, the system is composed of freely rotating chains. The contributions to the total energy of the system from the three sources described above have the following forms:

$$V_M(r) = A[1 - \exp - B(r - C)]^2 \tag{1}$$

$$V_H(r) = \tfrac{1}{2}k_0(\theta - \theta_0)^2 \tag{2}$$

$$V_B(r) = D \exp(-r/\rho) - Fr^{-6} \tag{3}$$

Bond energies, vibrational and structural data were used to derive the potential parameters corresponding to the above functional forms. Their values are gathered in Table 1. They have been tested previously in static simulations and they lead to structures that are in good agreement with experiment [2].

2.2 Results

Velocity autocorrection functions for both carbon and hydrogen atoms have been evaluated,

$$C(t) = \langle v(t) \cdot v(0) \rangle / \langle v(0)^2 \rangle \tag{4}$$

where $v(t)$ is the vector velocity of a given particle at a time t, and $\langle \ldots . \rangle$ stands for an average over all the particles belonging to the same species and over several time

Table 1 Potential parameters for the pristine PA. C is the commonly accepted length of each bond (distances in Angstroms, angles in degrees and energies in eV).

Interaction	*Type of potential*	*A*	*B*	*C*
C–C	Morse	4.5873	1.93	1.446
C=C	Morse	5.306	2.13519	1.346
C–H	Morse	4.3051	1.90291	1.08
		K_0	θ_0	
C–C=C	Harmonic	12.42	125.3	
C–C–H and C=C–H	Harmonic	5.2421	117.35	
		D	ρ	F
C . . . C	Buckingham	3627.4127	0.2778	24.6367
C . . . H	Buckingham	380.2212	0.2725	5.4218
H . . . H	Buckingham	115.116	0.2624	1.1841

origins. The Fourier transforms of these functions are useful to analyse the actual frequencies of motion. These power spectra are evaluated according to the expression

$$f(\omega) = \int_0^\infty c(t) \cos \omega t \, \mathrm{d}t. \tag{5}$$

These functions are displayed in Figure 2. The most relevant peaks are listed in Table 2 together with the experimental values reported in the literature from Raman [14] and infrared spectra [15] measurements and with the assignments to particular vibrational modes made by the authors. It is apparent that our results are in good agreement with experiment.

From the shape of the function $f(\omega)$ for the hydrogen atoms, it is apparent that the most important vibrational frequency for the hydrogen atoms comes from the C—H bond described by a Morse potential. Although this frequency appears in the carbon spectrum too, some other vibrational modes have greater intensities and, consequently, have a stronger influence on the overall motion of this type of atom. For instance, this is the case with the peaks corresponding to the C-C and to the C=C stretching modes.

Table 2 Relevant peaks in the lower spectra of PA. The parenthesis denote weak peaks.

v (cm^{-1})	*from Simulation*	*v (cm^{-1})*	*from Experiment**	
$f(\omega)$ Carbon	$f(\omega)$ Hydrogen			
100	100			
	330			
475			450	C—C—C deformation
790	790		750	C—H out-of-phase deformation (cis)
1130				
1240	(1240)			
1290	1290		1294	C—H in-plane deformation
1395	(1395)	1292		C—C stretch
1500	(1500)	1464		C=C stretch
	1760			
2050	2050			
3400	3400		3013	C—H stretch

* See references (14) and (15).

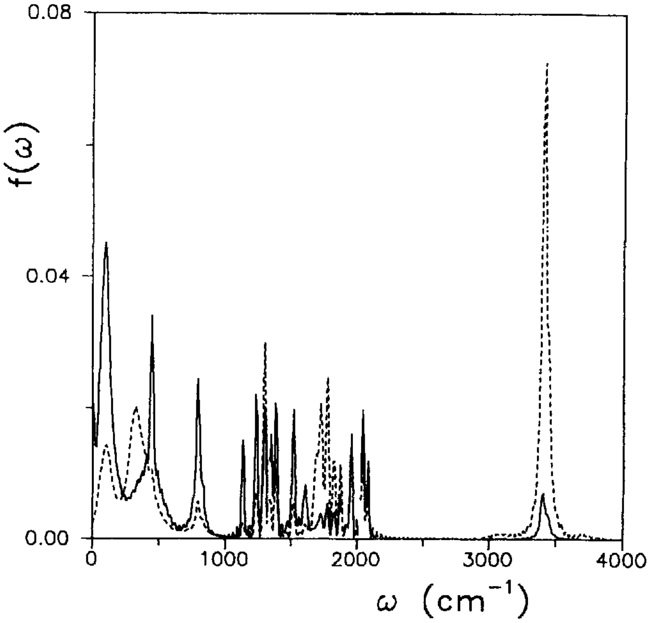

Figure 2 Power spectra of carbon and hydrogen in pristine PA. ——, $f(\omega)$ for carbon; - - -, $f(\omega)$ for hydrogen.

We have assigned these two modes to the frequencies 1395 cm^{-1} and 1500 cm^{-1} respectively. They appear also in the hydrogen spectrum, but the corresponding intensities are much lower.

We have calculated the mean square displacements for both the carbon and the hydrogen atoms, defined by

$$\mathbf{r}^2(t) = \langle |\mathbf{r}(t) - \mathbf{r}(0)|^2 \rangle \tag{6}$$

where $\mathbf{r}(t)$ is the position of a given particle at a time t and $\langle \ldots \rangle$ denotes the average over all the particles. This function is independent of the time origin and is related to the self-diffusion coefficient by the well-known equation [16]

$$D = \lim_{t \to \infty} \frac{1}{6t} \langle |\mathbf{r}(t) - \mathbf{r}(0)|^2 \tag{7}$$

The mean square displacement obtained for the carbon atoms reveals that the chains diffuse. The diffusion is mainly along the z axis. Similar behaviour is observed for the hydrogen atoms. As the value of the momentum of the system is zero, it is clear that not all the chains diffuse in the same direction. In support of our results it has been found, using minimisation techniques, that that activation energy for the translation of the chains is close to the thermal energy [17]. Nevertheless, this diffusion effect has not been detected experimentally. We attribute this to the presence of defects in real systems which may hinder this motion, for instance the cross-linking of the chains, a common feature in PA samples [18].

Table 3 Potential parameters for doped PA (distances in Angstroms, angles in degrees and energies in eV).

Interaction	*Potential*	*Parameters*
C . . . Li	Lennard-Jones	$A_1 = 872.1702 \quad B_1 = 24.5863$
H . . . Li	Lennard-Jones	$A_2 = 10.3641 \quad B_2 = -10.6642$
Li . . . Li	Repulsive term of the Buckingham	$A_3 = 1153.8 \quad \rho_3 = 0.1364$
C . . . K	Buckingham	$A_4 = 27135 \quad \rho_4 = 0.26905 \quad B_4 = 245$
H . . . K	Lennard-Jones	$A_5 = 10.3641 \quad B_5 = -64.7339$
K . . . K	Buckingham	$A_6 = 3796.9 \quad \rho_6 = 0.2603 \quad B_6 = 44.6$

3 LIGHTLY DOPED POLYACETYLENE

3.1 Model and Computational Details

In these calculations, the previously studied sample of pristine PA was doped with two lithium atoms. Our model assumes that the lithium atoms ionize and that there is a complete transfer of their charges to the carbon atoms in the chains, in such a way that the electrical neutrality of the system is maintained. The lithium atoms become Li^+ cations; no electrical charge has been assigned to the hydrogen atoms and every carbon in the system will have a fractional charge of $-1/96e$. In addition, the alternation of the bonds between the carbon atoms in the chains is replaced by a uniform set of bonds.

All the bonded interactions between carbon atoms are calculated using a Morse potential whose parameters have been derived by Corish *et al.* [3]. They used force constants derived from spectroscopic data on benzene [19] and by weight-averaging ethane and ethylene CC bond enthalpies [20] to the π-bond order of benzene. The potentials used to calculate both the two-body and three-body interactions between C and H are the same as for the pristine system. The potentials related to the Li^+ are

$$V_{\text{C-Li}}(r) = (1/96e)e/r + A_1 r^{-12} - B_1 r^{-6} \tag{8}$$

$$V_{\text{H-Li}}(r) = A_2 r^{-12} - B_2 r^{-6} \tag{9}$$

$$V_{\text{Li-Li}}(r) = e^2/r + A_3 \exp - (r/\rho_3) \tag{10}$$

where the parameters A_1, A_2, B_1 and B_2 have been calculated from data on the interaction energies of several hydrocarbons [21], and A_3 and ρ_3 were obtained by fitting to the elastic constants of several inorganic compounds [22]. The values of all these parameters are gathered in Table 3.

The simulations have been performed under the same thermodynamic conditions as the ones considered in the study of pristine PA. The system has been studied for 200 ps after an equilibration period of 3 ps. The initial configuration of the polyacetylene chains was out-of-phase as reported for the pristine system and the two Li^+ were intercalated in different "channels".

The dynamical behaviour of the chains is similar to that observed in pristine PA. To study the extent to which the dopant's motion depends on the motion of the chains and to separate both effects, we have performed another simulation in which the translation of PA was stopped by increasing the mass of one of the carbons in every chain by a factor of 10^5. This does not fix completely the PA chains, as it allows the energy exchange between them and the dopants.

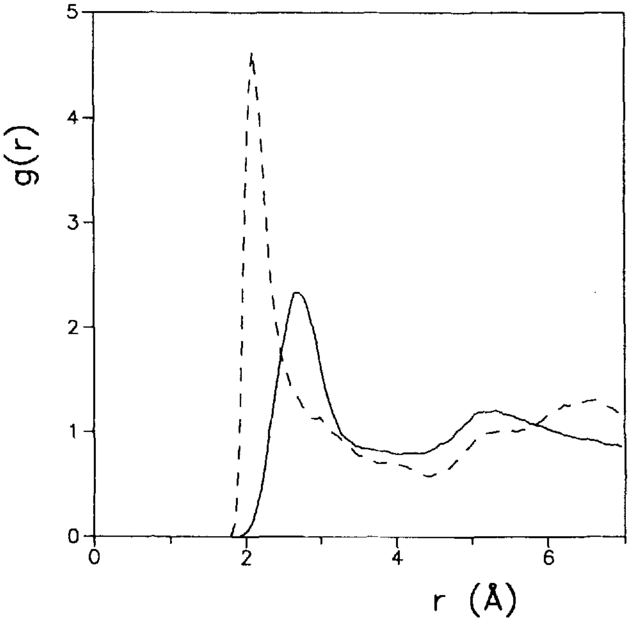

Figure 3 Radial distribution functions in lightly doped PA. ——, $g_{\text{C-Li}}(r)$; – – –, $g_{\text{H-Li}}(r)$.

3.2 Results

The partial radial distribution functions, related to the spatial distribution of the atoms, have been calculated. In Figure 3 we have plotted the radial distribution functions for C–Li and for H–Li. Both functions are liquid-like and from the position of the first maximum it is possible to assess that, on average, a lithium ion is closer to a carbon than to a hydrogen atom. These two $g(r)$ differ markedly from that for Li–Li, which is zero everywhere except for a very narrow zone of interparticle separations. This means that the distance between the two lithium ions is almost constant. As the electrostatic interaction between Li^+ is the strongest force in the system, to reach a minimum in the potential energy it is necessary to minimize this interaction. So the peak in the Li–Li radial distribution function corresponds to the maximum possible mean lithium separation for the concentration used in the simulation.

Examination of the dynamics shows that the motions of the two Li^+ ions are very much correlated, as is clear from Figures 4(a) and (b), where the evolution in time of their three coordinates are displayed. In particular, the qualitative evolution of the z coordinate shows remarkable similarities for both Li^+ ions. It is also apparent in the figure that they move quite freely along the axis of the chains (z axis), but their motion is more restricted in other directions.

The mean square displacement (6) has been calculated for the Li^+ ions. In Figure 5 we have plotted the results obtained in the simulations both where the chains are allowed to diffuse and where the polymer chains are clamped. There is a strong correlation between the diffusion of the chains and that of the ions in that no diffusion

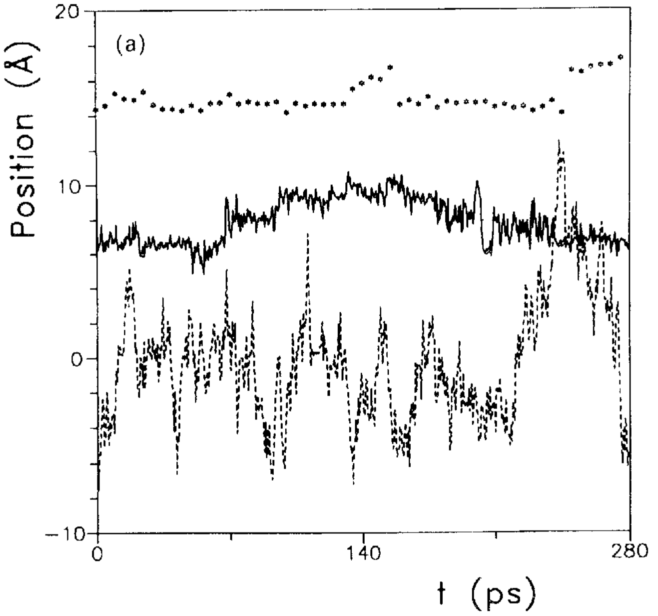

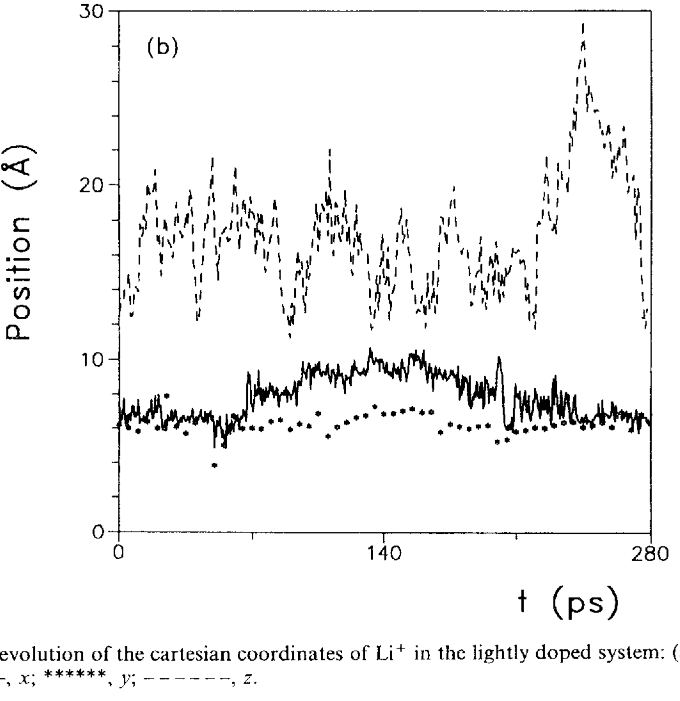

Figure 4 Time evolution of the cartesian coordinates of Li^+ in the lightly doped system: (a) for Li 1 and (b) for Li 2. ——, *x*; ******, *y*; – – – – – –, *z*.

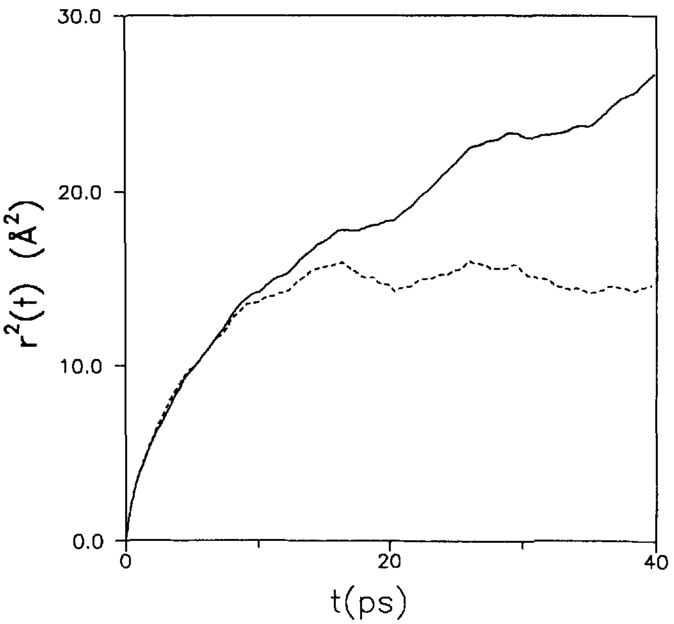

Figure 5 Mean square displacement for Li^+ in lightly doped PA. ——, with diffusing chains; - - - - - -, with clamped chains.

of the chains results in a very small diffusion coefficients for the ions, as was experimentally [23] obtained.

4 POTASSIUM DOPED POLYACETYLENE

4.1 Computational Details

Potassium has also been considered as a dopant for PA. The results of diffraction studies reported in the literature describe two quite different structures for PA when doped with alkali metal ions. Taking into account the results of a previous study that obtained the most stable structure of the host polymer after energy minimisation of the system [2], we will start our simulations from a structure in which the PA chains form slightly distorted square channels in which the metal ions occupy axial sites. These sites are located between the polymer chains to give effective intercalation into the PA. The dimensions of the unit cell are the ones reported by Baughman *et al.* [24]. The projections of it onto the planes parallel and normal to the channel directions are displayed in Figure 6.

We investigated two different dopant levels of potassium-doped PA. The first, called PAK1, has a potassium over the centres of alternate C—C bonds along each polymer corresponding to $(CHK_{0.25})_x$, which is the maximum experimentally measured doping of PA with sodium [25]. The second structure, PAK2, has overall composition $(CHK_{0.125})_x$, i.e., half the doping of PAK1. It corresponds more closely to the composition $(CHK_{0.18})_x$ with the highest concentration observed in potassium-doped PA.

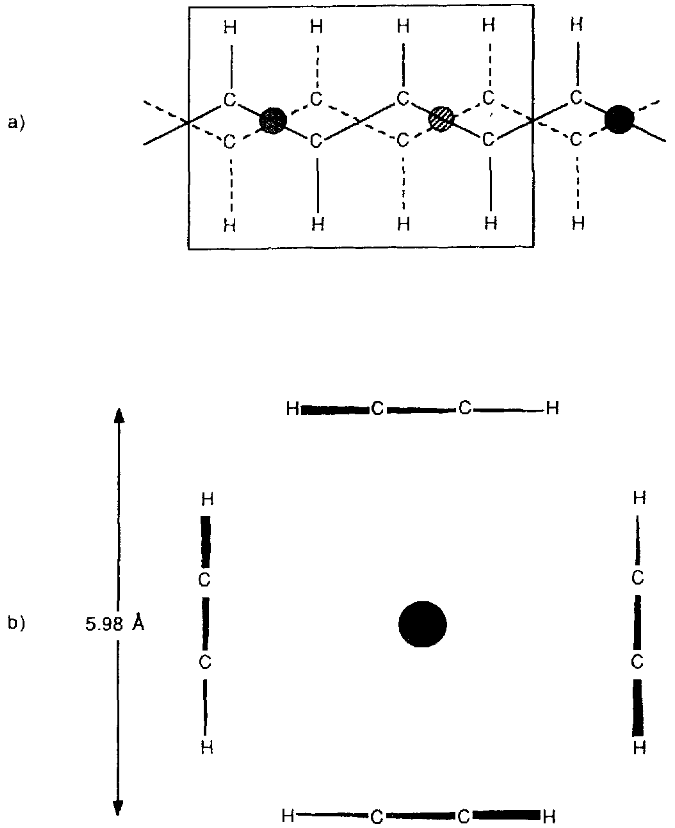

Figure 6 Unit cell of potassium-doped PA, projected on planes (a) parallel, and (b) normal, to the channel direction (*c*) axis). The filled circles represent K^+ ions. In PAK1 there would be dopant ions at both sites shown in the unit cell; in PAK2 only one site would be occupied.

As for the electrostatic interactions, we assume a complete transfer of the 4*s* electron of the potassium to the PA, leaving a set of K^+ cations. The charge transferred from a potassium atom is distributed equally amongst the carbon atoms in the system. Thus, the fractional charge will be $-0.25e$ in PAK1 and $-0.125e$ in PAK2.

Both, the three-body and the two-body interaction potentials between C and H are those used in the earlier sections of this paper. The interactions involving potassium were evaluated using the following functions

$$V_{\text{C-K}}(r) = qe/r + A_4 \exp(-r/\rho_4) - B_4 r^{-6} \tag{11}$$

$$V_{\text{H-K}}(r) = A_5 r^{-12} - B_5 r^{-6} \tag{12}$$

$$V_{\text{K-K}}(r) = e^2/r + A_6 \exp(-r/\rho_6) - B_6 r^{-6} \tag{13}$$

where q is the formal charge of the carbons in the chains. The parameters A_4 and B_4 have been calculated by a fitting procedure using the elastic constants of several inorganic compound [22]; A_4 and B_5 were derived by Corish *et al.* [2] who optimized the values obtained by Portman *et al.* [21] to the cell dimensions of Baughman *et al.*

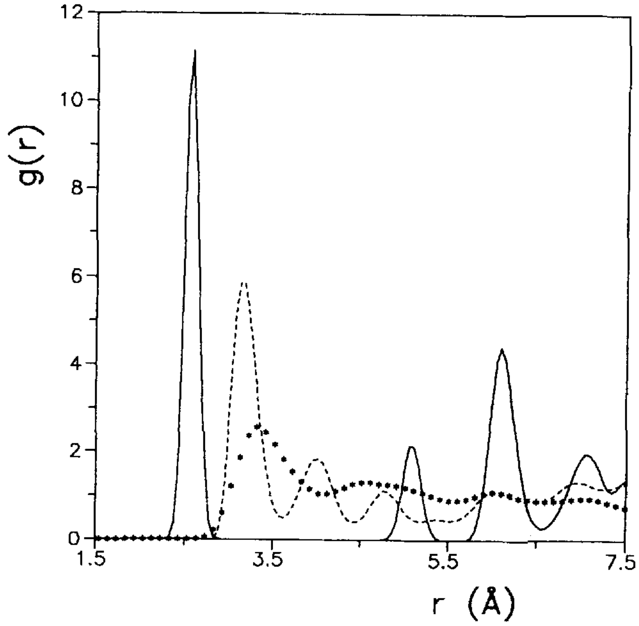

Figure 7 Radial distribution functions in PAK1. ——, $g_{K\ldots K}(r)$; ------, $g_{C\ldots K}(r)$; ******, $g_{H\ldots K}(r)$.

[24]. A_6 and B_6 were fitted to the results of a large number of *ab initio* calculations on organic systems [21]. All the corresponding numerical values are to be found in Table 3.

The dimensions of the two simulation boxes were 17.08 Å in the x and y directions and 14.88 Å in the z direction. The PA chains were parallel to the z direction. The total number of atoms was 432 in in PAK1 and 408 in PAK2. In both cases, the system was equilibrated at 300 K after an equilibration period of 2 ps. To achieve similar statistics in the functions where potassium is involved, PAK1 was studied during 200 ps and PAK2 during 300 ps. The cutoff for the short range two-body potentials, the integration algorithm and the timestep used in these simulations are the same as in all the previous studies.

4.2 Results

Partial radial distribution functions have been evaluated. $g_{H\ldots K}(r)$ $g_{C\ldots K}(r)$ and $g_{K\ldots K}(r)$ in PAK1 and in PAK2 and are displayed respectively in Figures 7 and 8. Whereas $g_{H\ldots K}(r)$ and $g_{C\ldots K}(r)$ are liquid-like, the $g_{K\ldots K}(r)$ have similarities with the radial distribution functions obtained in solid systems. In both cases we can refer to the potassium set of ions as to a "potassium sublattice", due to the well established positions for the potassium ions.

In addition, the structure shown in Figure 7 for the potassium sublattice in PAK1 is well approximated by the initial structure, but this is not the case with PAK2. The first peak of $g_{K\ldots K}(r)$ in Figure 8 corresponds to the distance between nearest neighbours in the same channel, and is the same as in the initial structure. The second peak, observed at 6.5 A, corresponds to the distance between nearest neighbours in adjacent channels. This distance is greater than it is in the initial configuration. Initially there

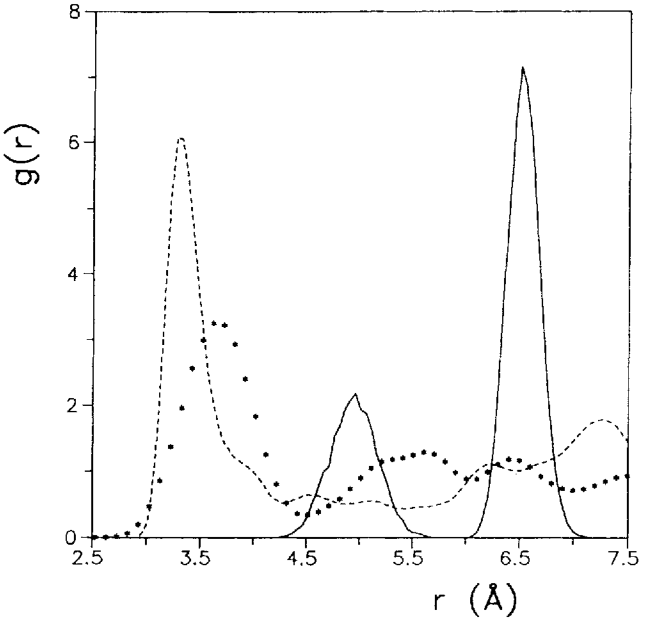

Figure 8 Radial distribution functions in PAK2. ——, $g_{K...K}(r)$; – – – – – –, $g_{K...K}(r)$; ******, $g_{H...K}(r)$.

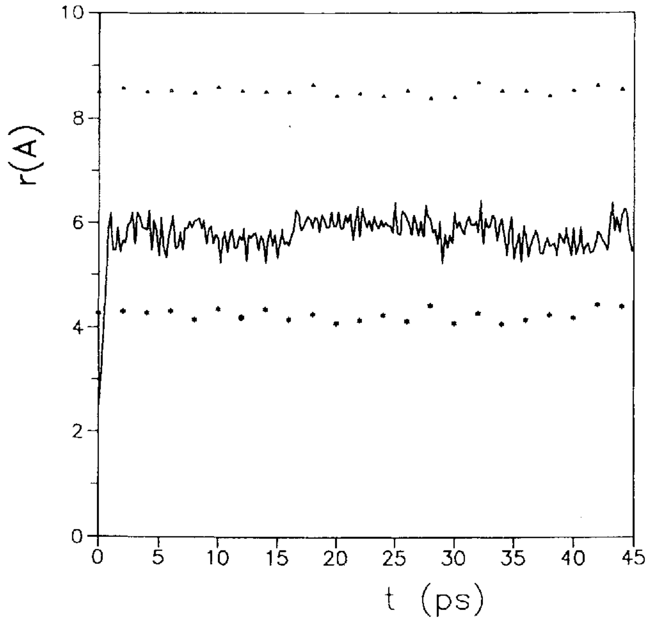

Figure 9 Time evolution of the cartesian coordinates of a K^+ in PAK1. ▲▲▲, x; ******, y; ——, z.

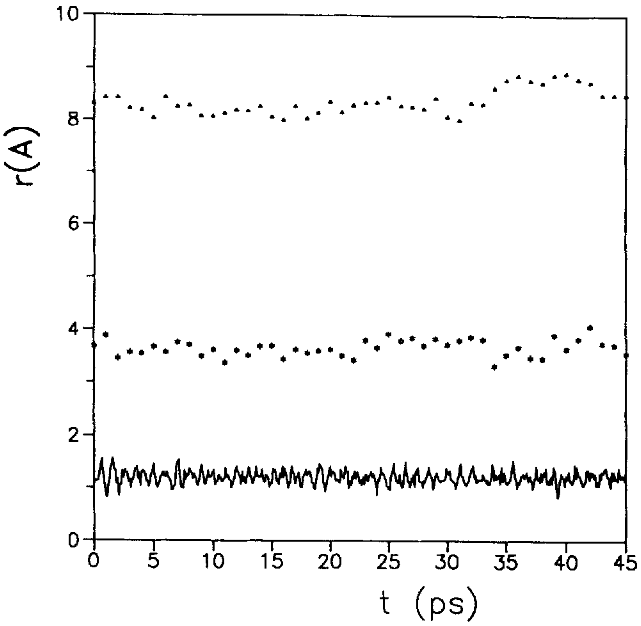

Figure 10 Time evolution of the cartesian coordinates of a K^+ in PAK2. ▲▲▲, x; ******, y; ——, z.

were three planes perpendicular to the polymer chains, each of them containing eight dopant ions. In the final structure, the dopants in adjacent channels tend to maximize their distances, locating themselves in different planes. Thus, the twenty-four dopants occupy six planes, four dopants in each of them.

In Figures 9 and 10 we have displayed the time evolution of a K^+ ion in PAK1 and PAK2 respectively. In PAK1, the motion in the direction of the axis of the chains has proved to have smaller amplitude than that in the x or y directions. The strong interactions between potassium ions force them to move as far as possible. In their motion, there is little tendency to move towards the next potassium ion but rather to approach the carbon atoms, which bear charges of the opposite sign. As the number of potassium ions in each channel is smaller in the semi-doped system (PAK2), the mobility of every K^+ in the direction of the chain's axis is bigger. Nevertheless, they show an oscillatory behaviour around the equilibrium positions corresponding to the peaks obtained in $g_{K \ldots K}(r)$.

5 SUMMARY

MD simulations have successfully simulated the structural and vibrational properties of pristine trans-polyacetylene. However, our simulations show high mobility of the polyacetylene chains which is probably not observed in the real systems owing to the presence of defects. In lightly Li doped polyacetylene, Li^+ ions are highly mobile parallel to the z axis, i.e. along the channels of the structure. This mobility is greatly reduced by clamping the carbon chains, showing that the dynamics of the Li^+ ions and of the chains are coupled. Simulations of semi-doped and fully-doped systems reveal a much more structured K sublattice with much lower mobilities of the K^+ ions.

Acknowledgements

We are grateful to the Commission of the European Communities for a grant (SCI 0174 C) supporting this work. We would like to thank Prof. J. Corish, Dr. D.A. Morton-Blake, Dr. V.C.A. Hanratty and Prof. F. Bénière for useful discussions. One of us (G.S.) wants to acknowledge the financial support from DGICYT, Project PB90-0613-CO3-01.

References

[1] R.B. Kaner and A.G. MacDiarmid, "Plastics that conduct electricity", *Scientific American*, February (1988).
[2] J. Corish, V.C.A. Hanratty, D.A. Morton-Blake, F. Benière and A. Morin, "Atomistic simulation calculations on the structures of conducting polymers. Part I. Pristine polyacetylene and polyparaphenylene", *J. Mol. Struct. (Theochem.)*, **207,** 41((1990).
[3] J. Corish, V.C.A. Hanratty, J.-P. Margritta, D.A. Morton-Blake, F. Benière and A. Morin, "Atomistic simulation calculations on the structures of conducting polymers. Part II. Doped polyacetylene and polyparaphenylene", *J. Mol. Struct. (Theochem.)*, **207,** 53 (1990).
[4] M.P. Allen and D.J. Tildesley, *Computer Simulation of Liquids*, Clarendon Press, Oxford (1987).
[5] S.W. De Leeuw, J.W. Perram and E.R. Smith, "Simulation of electrostatic systems in periodic boundary conditions. I. Lattice sums and dielectric constant", *Proc. R. Soc. London*, **A373,** 27 (1980).
[6] J.C.W. Chien, *Polyacetylene: Chemistry, Physics and Material Science*, Academic Press (1984).
[7] F. Benière, D. Boils, H. Cánepa, J. Franco, A. La Corre and J.P. Louboutin, "Polyacetylene solid-state batteries", *J. Electrochem. Soc.*, **132,** 21100 (1985).
[8] W.-P. Su, J.R. Schrieffer and A.J. Heeger, "Solitons in PA", *Phys. Rev. Lett.*, **42,** 1698 (1979); "Soliton excitations in PA", *Phys. Rev. B*, **22,** 2099 (1980).
[9] A.J. Heeger, S. Kivelson, J.R. Schrieffer and W.-P. Su, "Solitons in conducting polymers", *Rev. Mod. Phys.*, **60,** 781 (1988).
[10] D. Moses, A. Denenstein, J. Chen, A.J. Heeger, P. McAndrew, T. Woerner, A.G. MacDiarmid and Y.W. Park, "Effect of nonuniform doping on electrical transport in trans-$(CH)_x$: Studies of the semiconductor-metal transition", *Phys. Rev. B: Condens. Matter*, **25,** 7652 (1982).
[11] J.C.W. Chien, F.E. Karasz and K. Shimamura, "An estimate of bond length alteration in trans-PA", *Makromol. Chem., Rapid Commun.*, **3,** 655 (1982).
[12] R.W. Hockney and J.W. Eastwood, *Computer Simulation Using Particles*, McGraw Hill, New York (1981).
[13] D. Rigby and R.J. Roe, "Molecular dynamics simulation of polymer liquid and glass. I. Glass transition", *J. Chem. Phys.*, **87,** 7285 (1987).
[14] H. Takeuchi, Y. Furukawa, I. Harada and H. Shirakawa, "Vibrational analysis of polyacetylene and copoly(acetylene + acetylene − d_2): in-plane vibrations of trans-polyene chains", *J. Chem. Phys.*, **84,** 2882 (1986).
[15] H. Shirakawa and S. Ikeda, "Infrared spectra of poly(acetylene)", *Polymer J.*, **2,** 231 (1971).
[16] J.P. Hansen and I. McDonald, *Theory of Simple Liquids*, Academic Press (1986).
[17] D.A. Morton-Blake and V.A.C. Hanratty, Private communication.
[18] G. Wegner, "Polymers with metal-like conductivity. A review of their synthesis, structure and properties", *Angew. Chem. Int. Ed. Engl.*, **20,** 361 (1981).
[19] L. Pietronero, S. Straessler and P. Horsch, "Bond length, bond strength and electron lattice coupling in carbon based systems", *Mol. Cryst. Liq. Cryst.*, **83,** 211 (1982).
[20] P.W. Atkins, *Physical Chemistry*, Oxford University Press, Oxford (1978).
[21] P. Portman, T. Maruizumi, M. Welti, M. Badertscher, A. Neszmelyi, W. Simon and E. Pretsch, "Pair potentials for the interaction energy of Li^+, Na^+, K^+, and NH_4^+ with organic molecules", *J. Chem. Phys.*, **87,** 493 (1987).
[22] C.R.A. Catlow, K.M. Diller and M.J. Norgett, "Interionic potentials for alkali halides", *J. Phys. C: Solid State Phys.*, **10,** 1395 (1977).
[23] F. Benière, J. Corish, M.E.G. Lyons, T. McCabe and A. Morin, "Diffusion of iodine in polyacetylene", *J. Electrochem. Soc.*, **137,** 2181 (1990).

[24] R.H. Baughman, N.S. Murthy and G.G. Miller, "The structure of metallic complexes of polyacetylene with alkali metals", *J. Chem. Phys.*, **79**, 515 (1983).

[25] B. François, N. Mermillod and Z. Zuppirolli, "Swelling of polyacetylene when doped by iodine or sodium", *Synth. Met.*, **4**, 131 (1981).